Stability of Helix-Rich Proteins at High Concentrations

Jianxin Guo,[‡] Nicholas Harn,[‡] Aaron Robbins,[§] Ron Dougherty,[§] and C. Russell Middaugh*,[‡]

Department of Pharmaceutical Chemistry and Department of Mechanical Engineering, The University of Kansas, 2030 Becker Drive, Lawrence, Kansas 66047

Received March 15, 2006; Revised Manuscript Received May 19, 2006

ABSTRACT: A number of techniques, including circular dichroism, FTIR, front face fluorescence, and UV absorption spectrophotometries, dynamic light scattering, and DSC, were used to directly measure the colloidal and conformational stability of proteins in highly concentrated solutions. Using bovine serum albumin (BSA), chicken egg white lysozyme, human hemoglobin A_0, and bovine fibrinogen as model proteins, the thermal transition temperatures of proteins in dilute and concentrated solutions were compared. At 10 °C, no significant differences in both secondary and tertiary structures were detected for proteins at different concentrations. When temperature was introduced as a variable, however, hemoglobin and fibrinogen demonstrated higher transition midpoints (T_ms) in concentrated rather than in dilute solutions ($\Delta T_m \sim 2-10$ °C). In contrast, lysozyme and BSA in concentrated solutions exhibit a lower T_m than in dilute solutions ($\Delta T_m \sim 2-20$ °C). From these studies, it appears that a variety of factors determine the effect of high concentrations on the colloidal and conformational stability of a particular protein. While the prediction of excluded volume theory is that high concentrations should conformationally stabilize proteins, other factors such as pH, kinetics, protein dynamics, and intermolecular charge−charge effects may affect the overall stability of proteins at high concentrations under certain conditions.

Proteins often exist in their physiological environment at high concentrations or in crowded environments. Hemoglobin, for example, is found in erythrocytes at concentrations exceeding 300 g/L, and serum albumin is present in blood in the range of 35−55 g/L. In addition, the development of recombinant proteins as therapeutic agents has led to the need for protein formulations with reduced dosing volumes and subsequently high concentrations (*1*). Despite the increasing relevance of highly concentrated protein solutions, the unfolding and aggregation of proteins at high concentrations are incompletely understood. In 1977, Ross and Minton demonstrated that dramatic nonideality arises in the thermodynamic activity of hemoglobin in salt solutions with increasing protein concentrations (*2*). Activity coefficients of highly concentrated hemoglobin solutions were shown to be more than 2 orders of magnitude greater than the actual concentration. The question therefore of the impact of such dramatic increases in activity on the structure, function, and stability of protein molecules arises.

Stability at high concentrations needs to be viewed in several different contexts. For example, changes in the secondary and tertiary structure of a protein reflect the delicate balance of forces that control conformational stability. In contrast, colloidal stability results from the nature of the interactions between proteins and their interaction with the solvent, with aggregation the most well described manifestation of such phenomena. The two are often coupled with conformational change leading to protein association.

Significant effort to better understand the effect of macromolecular crowding on protein stability has been expended (*3*−*11*). Excluded volume theory predicts that high concentrations of inert macromolecular cosolutes will shift the equilibrium toward compact native states and away from less compact unfolded or partially folded forms (e.g., conformational stabilization) (*3*, *12*−*14*). Inert cosolutes refer to species of macromolecules that do not interact specifically with proteins. Excluded volume effects are derived from the mutual impenetrability of macromolecules, steric repulsion. Tellam et al. reported that the addition of the inert water-soluble polymer polyethylene glycol 6000 to a concentration of 100 g/L increased the unfolding temperature of G-actin by more than 5 °C. They attributed this effect to a stabilization of the native state by the excluded volume (*15*). Moreover, excluded volume theory predicts that self-association and hetero-association reactions will be facilitated in crowded fluids (*4*). Several reports have documented the enhancement of homo-oligomer formation by inert macromolecules (*10*, *16*, *17*). Thus, in light of excluded volume theory, the conformation stability of proteins at high concentration is thought to increase while colloidal stability decreases.

Proteins, however, are not inert macromolecules. By stressing a protein, we find the compact native conformation, with its well-defined secondary and tertiary structures, may become altered (e.g., more flexible) and potentially more interactive with other proteins. The degree to which this occurs is both concentration- and temperature-dependent, among other relevant variables. In dilute solutions, the stability of a protein is largely dictated by intramolecular

* To whom correspondence should be addressed: Department of Pharmaceutical Chemistry, The University of Kansas, 2030 Becker Dr., Lawrence, KS 66047. Telephone: (785) 864-5813. Fax: (785) 864-5814. E-mail: middaugh@ku.edu.

[‡] Department of Pharmaceutical Chemistry.

[§] Department of Mechanical Engineering.

10.1021/bi060525p CCC: $33.50
Published on Web 06/21/2006

interactions and hydration effects. At high concentrations, however, protein−protein interactions begin to contribute to protein stability. It is also possible that intramolecular interactions, including apolar and electrostatic effects, hydrogen bonds, and van der Waals forces, might be altered at higher protein concentrations. In addition, covalent alterations, including deamidation and oxidation, rupture of peptide bonds, and cleavage of disulfide bonds, are also concentration-dependent. All such phenomena potentially complicate our understanding of the colloidal and conformational stability of proteins at high concentrations when external stress is applied.

The effect of concentration on protein stability is not well understood partially because detailed studies of protein unfolding and aggregation mechanisms have traditionally been performed at low concentrations (<1 mg/mL). The extent to which such studies can be extrapolated to more concentrated conditions, however, remains to be clearly established. Methods that can directly probe the stability of proteins at high concentration are thus necessary, because any change in concentration as a result of dilution may alter a protein's physical state in a way that no longer represents the original physiological environment or the high concentrations necessary for certain technological and pharmaceutical applications.

In this work, a variety of biophysical approaches are adapted to characterize the comformational and colloidal stability of proteins directly in highly concentrated solutions. Using bovine serum albumin, chicken egg white lysozyme, human hemoglobin A_0, and bovine fibrinogen as model proteins, the thermal transition temperatures of proteins in dilute and concentrated solutions are compared. Tertiary structure changes are probed by front face fluorescence and short path length UV[1] absorption spectrophotometry. Secondary structure changes are investigated by short path length circular dichroism and attenuated total reflectance Fourier transform infrared spectroscopy (ATR-FTIR). Differential scanning calorimetry (DSC) is also employed to directly examine thermal transitions. In addition, colloidal stability is assessed by turbidity changes and dynamic light scattering. The method employed here suggests that the stability of proteins at high concentrations is as predicted driven at least partially by excluded volume effects. Excluded volume does not, however, explain some of the observed behavior, and therefore, other factors such as kinetics, dynamics, (non) specific interactions, and chemical degradation may be involved to varying degrees (*18*, *19*).

MATERIALS AND METHODS

Materials. Chicken egg white lysozyme (L7651), bovine serum albumin [A0281 (99% pure) and A4503 (96% pure)], human hemoglobin A_0 (H0267), and bovine fibrinogen (F4753) were purchased from Sigma Chemical Co. (St. Louis, MO). Lysozyme and bovine serum albumin (BSA) were supplied as essentially salt-free lyophilized powders and were used without further purification. Hemoglobin and fibrinogen contained large amounts of salts and stabilizers. They were therefore extensively dialyzed against the indicated buffer before being used. Dialysis cassettes (molecular weight cutoff of 10,000) were obtained from Pierce Biotechnology Inc. (Rockford, IL). A syringe-driven filter unit (0.22 and 0.45 μm) was obtained from Millipore (Bedford, MA). All reagents and chemicals (sodium phosphate monobasic, sodium phosphate dibasic, and sodium chloride) were ACS-grade or higher. Solutions were prepared using distilled, deionized water.

Preparation of Protein Solutions. Concentrated lysozyme solutions were prepared in phosphate buffer (10 mM, pH 7.4) and filtered. Because the buffering capacity of the protein became significant at high protein concentrations, the final pH of lysozyme at 350 mg/mL was 4.2. Fibrinogen stock was prepared in distilled, deionized water and dialyzed against NaCl-containing phosphate buffer [10 mM sodium phosphate and 0.5 M NaCl (pH 7.4)]. Hemoglobin and BSA stock solutions were prepared in distilled, deionized water and dialyzed against 10 mM phosphate buffer at pH 7.4 and 5.6, respectively. Although 99% pure BSA was used in the experiments reported here, in some cases, a less pure form was explored as discussed in the text. Nitrogen was bubbled during the dialysis process to prevent the oxidation of hemoglobin. Fibrinogen, hemoglobin, and BSA were filtered and concentrated by centrifugation after dialysis. To prepare proteins at low concentrations, the concentrated lysozyme solution was diluted with phosphate buffer (10 mM, pH 4.2) to match the apparent pH of the concentrated solutions. Since the pH of the solutions remained the same after dialysis, concentrated fibrinogen, hemoglobin, and BSA solutions were all diluted with the dialysis buffers. Potential pH changes of the protein solutions with temperature were measured. In all four concentrated solutions, the pH values dropped approximately 0.1−0.2 pH unit during the melting process, while the pH did not change in dilute solutions. The concentrations of the proteins were determined using diluted solutions, the published extinction coefficients, and A_{280} measurements. As specified below, all dilute condition studies were performed with a protein concentration of <1 mg/mL. The high concentrations that were used were the highest that could be attained without visible aggregation of the protein.

Dynamic Light Scattering. Experiments were conducted using a custom-built system utilizing the one-beam method for multiple scattering suppression (*20*, *21*). A Spectra-Physics argon ion laser, which was set to a wavelength of 514.5 nm, was employed and powered around 0.1 W. The PMTs and correlator were purchased from correlator.com and use the real-time program Flex 5000 to acquire the scattering data. All studies were conducted at a temperature of 15 °C which was maintained using a cooled water bath.

The samples were tested for multiple scattering using the one-beam method by adjusting the tilt angle up to 3−4 mrad between two detectors and cross correlating the two scattering signals. Each protein was tested at varying concentrations, and data were acquired for 60−500 s depending on the tilt angle of the detector (a longer time for a longer tilt angle). The data were analyzed using two programs: Flex 5000 and CONTIN. Flex 5000 uses a cumulant method to solve for the diameter, while CONTIN uses a method that involves taking the inverse Laplace transform of the data. Two CONTIN solutions are provided; the first CONTIN solution

[1] Abbreviations: ATR-FTIR, attenuated total reflectance Fourier transform infrared spectroscopy; UV, ultraviolet; DSC, differential scanning calorimetry; T_m, transition midpoint; BSA, bovine serum albumin; OD, optical density; CD, circular dichroism.

is a least-squares fit to the correlation function, while the second solution is considered to be the best possible solution to the data. This "best possible fit" is determined by adjusting a regularization parameter so that the size distributions are not overly narrowed or widened upon fitting (*22*−*24*). The second solution is reported here because of experience with the quality of the solution and because the determined values were closest to those previously reported for these proteins in dilute solutions (*25*, *26*). All measurements are the average of at least three trials ± the standard deviation.

Derivative UV Absorbance Spectroscopy and Turbidity. UV absorbance temperature perturbation studies were conducted with an Agilent (Palo Alto, CA) 8453 diode array UV−visible spectrophotometer. Spectra were collected over a temperature range of 10−85 °C at 2.5 °C intervals. The effect of temperature on protein aggregation was studied by monitoring the turbidity at 350 nm (OD_{350}). A 1 cm path length cuvette was used with a total sample volume of 0.2 mL for proteins at dilute concentrations. A 0.01 cm path length cuvette was used for concentrated fibrinogen (59 mg/mL), and a 0.001 cm path length cuvette was used for concentrated lysozyme (350 mg/mL), hemoglobin (245 mg/mL), and BSA (330 mg/mL). Since no significant differences in spectral changes were seen at equilibrium times between 1 and 5 min, a 1 min equilibrium period was employed before collection of data at each temperature. Spectral analysis was conducted using Chem-station (Agilent). Second-derivative spectra were calculated using a nine-point data filter, fifth-degree Savitzky−Golay polynomial and were subsequently fitted to a cubic function with 99 interpolated points per raw data point. The calculation of the second-derivative spectrum in this manner permitted 0.01 nm resolution, as described previously (*27*). Peak positions were determined from the interpolated curves using Microcal Origin 7.0. Transition midpoints were determined with a fit to a sigmoidal function or by first derivatives of the transitions for nonsigmoidal fits using Microcal Origin 7.0.

Fluorescence Spectroscopy. Fluorescence spectroscopy employing front face sampling geometry was used to probe changes in the tertiary structure of the proteins at high concentrations as a function of temperature. The use of a right angle triangular cuvette was necessary because of the extreme inner filter effect present at high concentrations (*28*, *29*). A rectangular cuvette, on the other hand, was used in dilute solutions. The only exception was fibrinogen, which was examined at low concentrations in the triangular cuvette due to its high extinction coefficient. An excitation wavelength of 295 nm was employed (>95% Trp emission), and emission spectra were recorded from 310 to 450 nm using a QuantaMaster spectrofluorometer equipped with a Peltier thermostated cuvette holder (Photon Technologies International, Lawrenceville, NJ). Data were collected every 0.5 nm at a scanning rate of 1 nm/s. Full spectra were obtained every 2.5 °C from 10 to 85 °C with a 5 minute thermal equilibration at each temperature. The data were processed, and peak positions were determined using Microcal Origin 7.0.

Circular Dichroism. CD spectra were recorded with a Jasco (Tokyo, Japan) J-720 spectrophotometer equipped with a Peltier temperature controller. Far-UV spectra were collected with 1 mm path length cuvettes sealed with a Teflon stopper for dilute protein solutions. An extremely short path length (0.5−5 μm) cell was made for proteins at high concentrations by dropping a small volume of protein solution (1−10 μL) on a quartz plate and sliding a second plate across its surface in a manner that allowed capillary action to fill the space between the plates. The path length was then determined by UV absorbance measurements. The ellipticity at 222 nm was simultaneously monitored at 0.1 °C intervals at a thermal ramp rate of 1 °C/min. Complete spectra were also collected at 10 °C and at the end of the melting process (i.e., 85 °C for lysozyme, BSA, and hemoglobin and 65 °C for fibrinogen). A data pitch of 0.5 nm and a scanning speed of 10 nm/min with a 2 s response time were used to acquire each spectrum. Data analysis was performed using Standard Analysis and Temperature/Wavelength Analysis (Jasco) and MicroCal Origin 7.0.

FTIR Spectroscopy. BSA (12 and 330 mg/ml), lysozyme (10 and 400 mg/mL), human hemoglobin A_0 (8 and 245 mg/mL), and fibrinogen (11 and 59 mg/mL) were used in this study. Higher concentrations were employed for the dilute comparison in this case due to the lower sensitivity of FTIR spectroscopy. Lysozyme was dissolved in 10 mM deuterated phosphate buffer, and the final pD was 4.2. Protein solutions in D_2O were placed at room temperature overnight to ensure extensive H−D exchanges. Because fibrinogen, BSA, and hemoglobin had to be dialyzed before use, they were examined by FTIR in aqueous solution. An ATR (attenuated total reflectance) cell equipped with a 45° ZnSe trough plate and sealed liquid cover was employed. Data were collected using 256 scans at a resolution of 4 cm^{-1} with a Nicolet Magna 560 FTIR spectrometer that was equipped with an MCT/A detector. A thermal ARK temperature controller (Spectra-Tech, Inc., Shelton, CT) was used to vary the temperature every 5 °C from 30 to 80 °C. The samples were equilibrated for 7 min at each temperature. Thermal melt spectra were acquired for the proteins and buffer solutions. Buffer spectra at each temperature were subtracted from the protein spectra using Grams AI version 7.0 (Thermo Galactic). The resulting data were copied into Microsoft Excel, and a ratio of the absorbance at two frequencies was calculated and plotted versus temperature.

Differential Scanning Calorimetry. Differential scanning calorimetry (DSC) was employed to determine the thermal transition temperatures (T_ms) of the proteins at different concentrations. A high-throughput capillary differential scanning calorimeter (MicroCal LLC, Northampton, MA) was used for proteins at lower concentrations. A scan rate of 60 °C/h was used to obtain data from 10 to 90 °C. A DSCQ100 (TA Instruments, New Castle, DE) was employed to measure T_m values for proteins at high concentrations. The modulated DSC mode was applied with a 60 s modulation period and a 60 °C/h ramp rate. Even though the MicroCal LLC measures heat capacity (kilocalories per mole per degree Celsius) and the DSCQ100 device monitors heat flow (milliwatts), the identical scanning rates that were employed permit direct comparison between the two calorimetric methods. In some cases, experiments were conducted at the same concentration (e.g., 10 mg/mL in the two different instruments) and gave essentially identical T_m values.

RESULTS

DLS

The hydrodynamic diameter of BSA, lysozyme, and fibrinogen was determined at low and high concentrations. Because only a weak scattering signal was observed in the concentrated hemoglobin solution due to absorption of the incident light even after the laser was adjusted to 1 W, results were not further analyzed. The size of BSA was determined to be 6.00 ± 0.43 nm at 10 mg/mL and 6.70 ± 0.29 nm at 280 mg/mL by employing a CONTIN analysis of the correlation function at zero tilt angle. The presence of multiple scattering can be identified by an approximate 10−20% increase in diameter with an increasing tilt angle of the detectors (*20*). BSA demonstrates an approximate 17% increase in diameter with an increasing tilt angle, but due to the uncertainty in the size measurement versus tilt angle even after evaluation of intermediate concentrations, the observed increase at higher concentrations cannot definitely be attributed to either multiple scattering or an increase in hydrodynamic diameter (data not illustrated). Fibrinogen, the largest of the four proteins that were tested, shows the most significant increase in diameter (∼5 nm) with an increasing tilt angle. Again, due to the uncertainty of the data obtained when the tilt angle is changed, it is not clear whether the sample exhibits multiple scattering. The sizes measured for fibrinogen were 22.81 ± 2.13 nm at 2 mg/mL and 34.45 ± 5.20 nm at 42 mg/mL. Lysozyme, the smallest of the proteins that were tested, did not exhibit any significant increase in diameter with an increasing tilt angle. Lysozyme at 10 mg/mL exhibited a diameter of 3.22 ± 0.63 nm and a diameter of 2.46 ± 0.21 nm at 350 mg/mL. Other intermediate concentrations produced size estimates that are between these two values but demonstrated no discernible trend. The sizes of all the proteins measured in dilute solutions are close to those previously reported (*25*, *26*).

UV Absorbance Spectroscopy

Aggregation of Proteins. Temperature-induced aggregation was studied by turbidity measurements (OD_{350}) acquired simultaneously with the absorbance data. Both concentrated lysozyme and fibrinogen aggregate more extensively than in dilute solutions as indicated by a large increase in OD_{350} with an increase in temperature (Figure 1A,C). Little or no aggregation is observed for lysozyme in dilute solutions. The temperature at which aggregation occurs for fibrinogen is the same at low and high concentrations (53 °C). The increase in the OD_{350} of hemoglobin at high concentrations is smaller than that in dilute solutions and occurs at a much higher temperature (∼10 °C higher, Figure 1B). Concentrated BSA forms a transparent gel when heated. Nevertheless, a small transition is still evident (inset of Figure 1D) which is 15 °C lower than that seen in dilute solutions. This result correlates well with the transitions seen in UV derivative absorbance spectroscopy (discussed below).

High-Resolution Derivative Absorbance Spectroscopy. The second-derivative UV absorbance spectrum of the four proteins that were studied exhibits four to six distinct negative peaks. At 10 °C, the six most common negative peaks of model aromatic amino acids occur at approximately 252.7 (peak 1, Phe), 258.8 (peak 2, Phe), 265.5 (peak 3, Phe), 277.6 (peak 4, Tyr), 283.9 (peak 5, Trp/Tyr), and 290.6 nm (peak 6, Trp) (*27*). The changes in peak positions with temperature at both a low and high concentration for the four proteins are summarized in Figures 2−5.

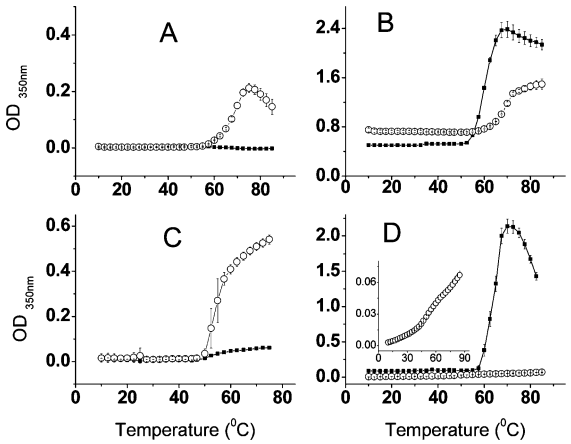

FIGURE 1: Comparison of thermal aggregation determined by optical density measurements at 350 nm in dilute (■) and concentrated (○) solutions: (A) lysozyme [(■) 0.41 and (○) 350 mg/mL], (B) hemoglobin [(■) 0.3 and (○) 245 mg/mL], (C) fibrinogen [(■) 0.17 and (○) 59 mg/mL], and (D) BSA [(■) 0.27 and (○) 330 mg/mL]. The inset shows an amplification of the data from 330 mg/mL protein. The error bars represent the standard error ($n = 3$). Error bars that are not visible are hidden within the symbol.

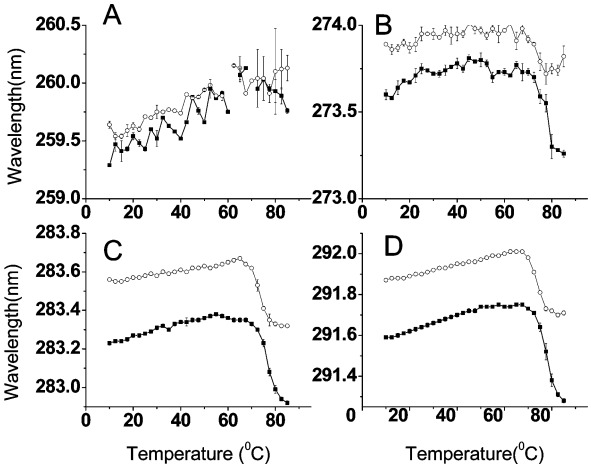

FIGURE 2: Derivative UV absorbance studies of lysozyme in dilute (■, 0.41 mg/mL) and concentrated (○, 350 mg/mL) solutions as a function of temperature: (A) Phe, (B) Tyr, (C) Tyr/Trp, and (D) Trp. The error bars represent the standard error ($n = 3$). Error bars that are not visible are hidden within the symbol.

Lysozyme. Only four peaks were resolved for lysozyme (Figure 2), arising from Phe, Tyr, Tyr/Trp, and Trp residues. Plots of peak position versus temperature exhibit clearly defined transitions induced by increases in temperature. The directions of the transitions were similar at both high and low concentrations, shifting to a lower wavelength at higher temperatures. Studies with model compounds in various solvents indicate that shifts to lower wavelengths correspond to movement into more polar environments (the opposite of that seen in fluorescence spectra) and vice versa (*30*). Thus, on the basis of shifts in peak positions, tyrosine and tryptophan residues become more exposed but to different extents upon heating (Figure 2B−D). In general, transition midpoints of lysozyme at high concentrations calculated from the individual peaks are ∼2 °C lower than those seen in dilute solutions (Table 1).

Table 1: Transition Midpoints (T_ms) of Proteins Determined by DSC, UV Absorbance, Fluorescence, and CD ($n = 3$)[a]

Protein	DSC	UV			OD_{350}	fluorescence		CD (°C)
		Tyr	Try/Trp	Trp		peak position	intensity	
lysozyme								
0.41 mg/mL	77.7 ± 0.02	75	75	76.7 ± 1.2	no transition	80	no transition	80
350 mg/mL	73.2	72.5	73.3 ± 1.2	73.3 ± 1.2	69.3 ± 0.4	75	72.5	74
hemoglobin								
0.3 mg/mL	67.0 ± 0.4	62.5	61.3 ± 1.3	63.8 ± 1.3	58.7 ± 0.6	NA[b]	NA[b]	73 ± 1.5
245 mg/mL	75 ± 0.7	64 ± 1	71 ± 2	72 ± 1	68.3 ± 1.2	NA[b]	NA[b]	73 ± 0.5
fibrinogen								
0.17 mg/mL	50.7 ± 0.2	50 ± 2.0	50	50	53.1 ± 1.1	42.5 ± 2.5	47.5	47.5
59 mg/mL	53.5 ± 0.1	51.9 ± 2.1	51.7 ± 1.2	52.5 ± 1.8	53.3 ± 1.2	50	47.5	50
BSA at pH 5.6								
0.27 mg/mL	72.3 ± 0.8	61.7 ± 2.4	62.5	62.5	65	47.5	52.5	75
330 mg/mL	52.6 ± 0.1	61.7 ± 1	55	45.8 ± 1	50	45 ± 2.5	42.5	57.5
BSA at pH 6.8								
0.36 mg/mL	78.5 ± 0.4	NA[b]	55.8 ± 1	55	no transition	55	55	60
340 mg/mL	55	NA[b]	55.8 ± 1	52.9 ± 1	54.2 ± 2	57.5	51.9 ± 0.6	60

[a] Where standard deviations are not shown, they are numerically zero. [b] Not available.

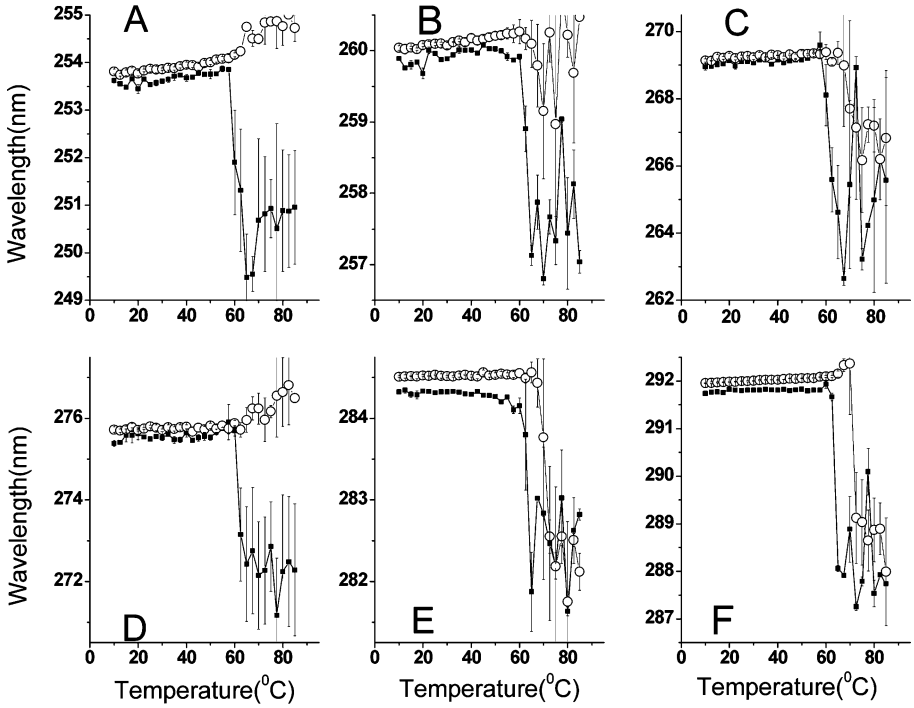

FIGURE 3: Derivative absorbance studies of hemoglobin in dilute (■, 0.3 mg/mL) and concentrated (○, 245 mg/mL) solutions as a function of temperature: (A) Phe, (B) Phe, (C) Phe, (D) Tyr, (E) Tyr/Trp, and (F) Trp. The error bars represent the standard error ($n = 3$). Error bars that are not visible are hidden within the symbol.

Hemoglobin. The second-derivative spectra exhibit six distinct negative peaks, most of which shift to lower wavelengths after the observed temperature transition at both concentrations (Figure 3). Hemoglobin in dilute solutions unfolds abruptly upon heating accompanied by irreversible aggregation. The aggregation is sufficiently extensive that it reduces peak resolution and produces noisy spectra despite the use of derivative analysis. Concentrated hemoglobin, on the other hand, is relatively stable, producing significantly greater melting temperatures (~9 °C higher).

Fibrinogen. In both dilute and concentrated solutions, fibrinogen manifests similar trends in tertiary structure change upon melting (Figure 4). The peaks of phenylananine, tyrosine, and tryptophan residues all shift to higher wavelengths after their transitions. In this case, a higher concentration produces an ~2 °C higher T_m.

BSA. Concentrated BSA gels at elevated temperatures, while significant precipitation is observed in dilute solutions. At 0.27 mg/mL, the first two derivative peaks of the Phe residues shift to lower wavelengths while the third shifts to higher wavelengths (Figure 5A−C). Tyr and Trp peak positions shift to higher wavelengths after the transition (Figure 5D−F). At 330 mg/mL, the Phe peak positions are unperturbed by temperature. Using this approach, BSA appears to be largely destabilized with the T_m 17 °C lower than that seen in dilute solutions (Figure 5F and Table 1).

Intrinsic Tryptophan Fluorescence

Lysozyme and hemoglobin possess six Trp residues each. Fibrinogen has approximately 40 Trp residues, while BSA possesses only two indole side chains, one embedded in each of its two domains. The heterogeneous placement, amount,

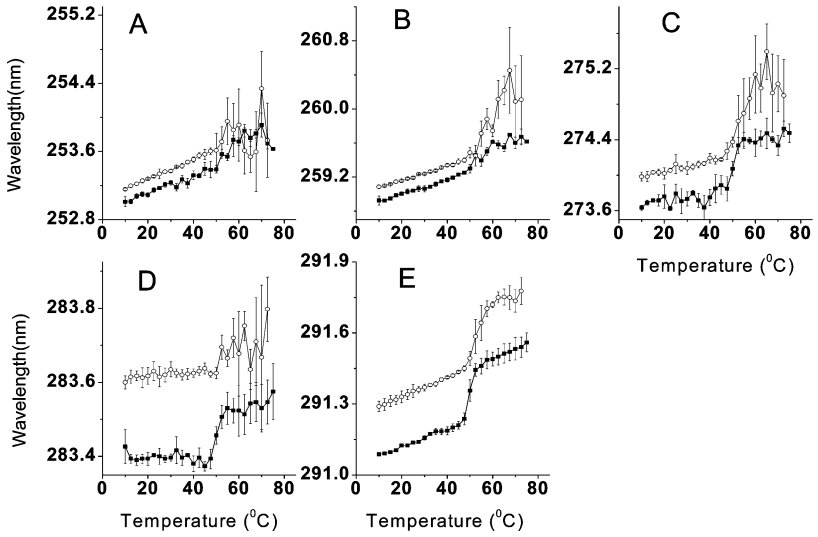

FIGURE 4: Derivative absorbance studies of fibrinogen in dilute (■, 0.17 mg/mL) and concentrated (○, 59 mg/mL) solutions as a function of temperature: (A) Phe, (B) Phe, (C) Tyr, (D) Tyr/Trp, and (E) Trp. The error bars represent the standard error ($n = 3$). Error bars that are not visible are hidden within the symbol.

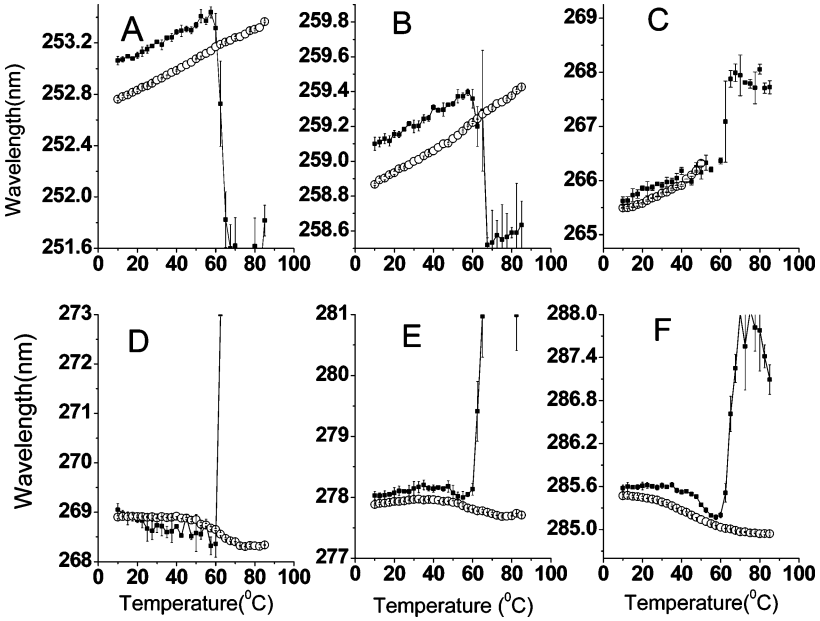

FIGURE 5: Derivative absorbance studies of BSA in dilute (■, 0.27 mg/mL) and concentrated (○, 330 mg/mL) solutions as a function of temperature: (A) Phe, (B) Phe, (C) Phe, (D) Tyr, (E) Tyr/Trp, and (F) Trp. The error bars represent the standard error ($n = 3$). Error bars that are not visible are hidden within the symbol.

and high extinction coefficient make tryptophan a good probe of these proteins' tertiary conformation (*31*, *32*).

Lysozyme. At 10 °C, the positions of the emission maxima for lysozyme in dilute and concentrated solutions are 336.8 ± 0.5 and 335.3 ± 1.2 nm, respectively (Figure 6A.i). The proximity of these values suggests that the Trp side chains are on average exposed to similar environments regardless of concentration. As the temperature is increased, the peak positions of the protein red shift at ~70 °C (Figure 6A.i). The T_m of the protein in dilute solution is approximately 5 °C higher (Table 1) than in the concentrated state.

The intensity of the tryptophan fluorescence in dilute solutions decreases continuously over the temperature range that was studied without an obvious transition (Figure 6A.ii). In contrast, a marked increase in intensity is seen at ~72.5 °C, concomitant with gel formation in the more concentrated solution.

Fibrinogen. The tryptophan residues of fibrinogen at high concentrations (emission maximum at 334 nm) exhibit a 3 nm blue shift at 10 °C compared to those in dilute solutions (emission maximum at 337.3 ± 0.3 nm) (Figure 6B.i). It has previously been reported that fibrinogen in solution undergoes concentration-dependent self-association at room temperature (*33*). The blue shift seen in the tryptophan peak position at high concentrations may reflect such an event with increased exposure to apolar environments of some Trp side chains. These data also correlate with DLS observations since the size of fibrinogen increases with concentration. While a gradual red shift is seen under dilute conditions, a much sharper transition occurs in concentrated solutions at higher temperatures. This red shift is in apparent contradiction to the UV absorption results where a red shift is also seen at higher temperatures. In a series of elegant studies, Vivian and Callis show that the positions of protein Trp

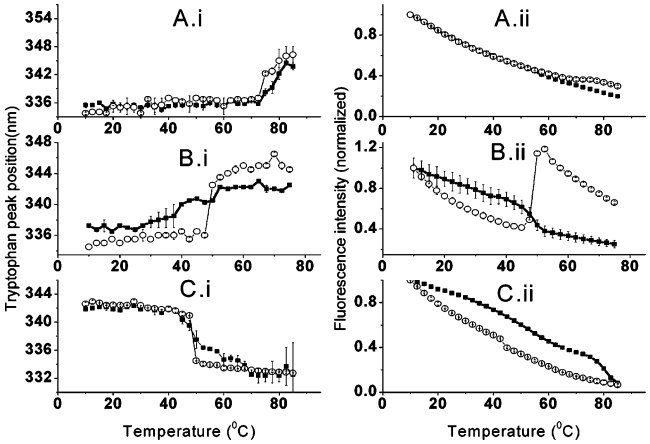

FIGURE 6: Comparison of tertiary structure stabilities determined by fluorescence spectroscopy of proteins in dilute (■) and concentrated (○) solutions. (A.i−C.i) Tryptophan peak position as a function of temperature. (A.ii−C.ii) Tryptophan fluorescence emission intensity at a fixed wavelength as a function of temperature: (A) lysozyme [(■) 0.41 and (○) 350 mg/mL], (B) fibrinogen [(■) 0.17 and (○) 59 mg/mL], and (C) BSA [(■) 0.27 and (○) 330 mg/mL]. The error bars represent the standard error ($n = 3$). Error bars that are not visible are hidden within the symbol.

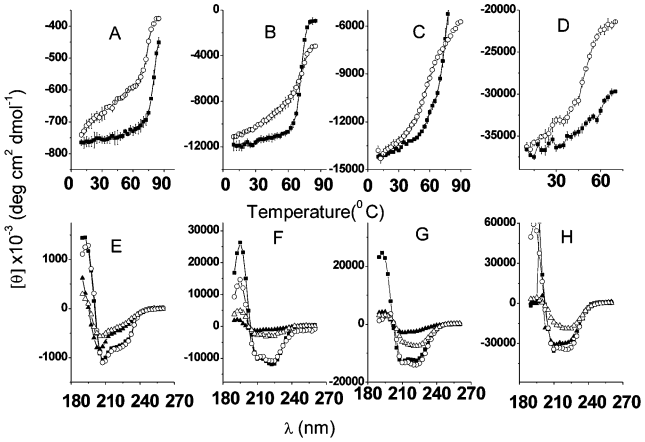

FIGURE 7: Comparison of secondary structure stabilities determined by CD. (A) Molar ellipticity at 222 nm of lysozyme in dilute (■, 0.41 mg/mL) and concentrated (○, 350 mg/mL) solutions as a function of temperature. (B) Molar ellipticity of hemoglobin at 222 nm in dilute (■, 0.3 mg/mL) and concentrated (○, 245 mg/mL) solutions as a function of temperature. (C) Molar ellipticity at 222 nm of BSA in dilute (■, 0.27 mg/mL) and concentrated (○, 330 mg/mL) solutions as a function of temperature. (D) Molar ellipticity of fibrinogen at 222 nm in dilute (■, 0.17 mg/mL) and concentrated (○, 59 mg/mL) solutions as a function of temperature. (E) Spectra recorded before [(■) 0.41 and (○) 350 mg/mL] and after melting [(▲) 0.41 and (△) 350 mg/mL] of lysozyme. (F) Spectra recorded before [(■) 0.3 and (○) 245 mg/mL] and after melting [(▲) 0.3 and (△) 245 mg/mL] of hemoglobin. (G) Spectra recorded before [(■) 0.27 and (○) 330 mg/mL] and after melting [(▲) 0.27 and (△) 330 mg/mL] of BSA. (H) Spectra recorded before [(■) 0.17 and (○) 59 mg/mL] and after melting [(▲) 0.17 and (△) 59 mg/mL] of fibrinogen. The error bars represent the standard error ($n = 3$). Error bars that are not visible are hidden within the symbol.

fluorescence emission peaks are a product of contributions from both the solvent and the protein matrix (*31*). In fact, the contribution from the protein itself can often be the dominating effect (see Figure 3 in ref *31*), resulting in either blue or red shifts depending on the nature of any change in the immediate electrostatic environment of each indole chromophore. Thus, the apparent contradiction between the direction of the shifts seen by UV absorption and fluorescence may reflect specific changes in the interaction of the fibrinogen protein backbone and side chains with their Trp fluorophores rather than be an immediate consequence of changes in solvent exposure.

Although the T_m value determined from intensity versus temperature plots occurs at the same temperature in dilute and concentrated solutions (48 °C), the intensity increases dramatically at high concentrations rather than decreasing as seen in dilute solution (Figure 6B.ii). This difference in intensity change may reflect the different properties of the sample upon heating, because fibrinogen forms heterogeneous precipitates in dilute solutions but homogeneous gels at high concentrations.

BSA. At 10 °C, BSA in dilute solution possesses an emission maximum at 342 nm, close to the value of 343 nm observed in concentrated solutions (Figure 6C.i). With an increase in temperature, the fluorescence emission peak of BSA in dilute solutions exhibits a transition at 47.5 °C to lower wavelengths. This transition occurs at 45 ± 2 °C for BSA at high concentrations. The fluorescence intensity decreases with temperature at both concentrations with a T_m of 52.5 °C in dilute solutions and 42.5 °C at high concentrations (Figure 6C.ii).

Hemoglobin. The fluorescence of hemoglobin at both concentrations could not be detected, despite the use of front surface geometry. This is probably due an extreme inner filter effect at high concentrations. We were also unable to obtain good fluorescence data from hemoglobin at 0.3 mg/mL presumably because of the reduced sensitivity of the front face geometry. Since very strong nonideality arises in the thermodynamic activity of hemoglobin with an increase in concentration, the extrapolation from two or three low-end concentrations to higher concentrations is not possible. Thus, comparative hemoglobin fluorescence results are unavailable.

Far-UV Circular Dichroism

The CD spectra of the four proteins undergo temperature-dependent transitions that are characterized by a large loss in helicity. Plots of ellipticity at 222 nm as a function of temperature exhibit sigmoidal curve shapes (Figure 7A−D). Secondary structure changes with temperature exhibit trends similar to those seen with tertiary structure alterations and are summarized in Table 1. At 10 °C, the proteins exhibit similar secondary structures at different concentrations, as indicated by their virtually identical CD spectra (Figure 7E−H).

Lysozyme. When the ellipticity at 222 nm is monitored with an increase in temperature, lysozyme at high concentrations exhibits a lower stability (~6 °C decrease) than in dilute solutions (Figure 7A).

Hemoglobin. There is no significant difference in the T_m values observed in the secondary structure changes of hemoglobin at different concentrations (Figure 7B). UV derivative absorbance spectroscopy and turbidity studies show that hemoglobin is stabilized by approximately 9 °C at high concentrations. The data suggest that hemoglobin in dilute solution precipitates rapidly with changes in tertiary structure occurring, while the secondary structure remains essentially intact at least in the protein remaining in solution.

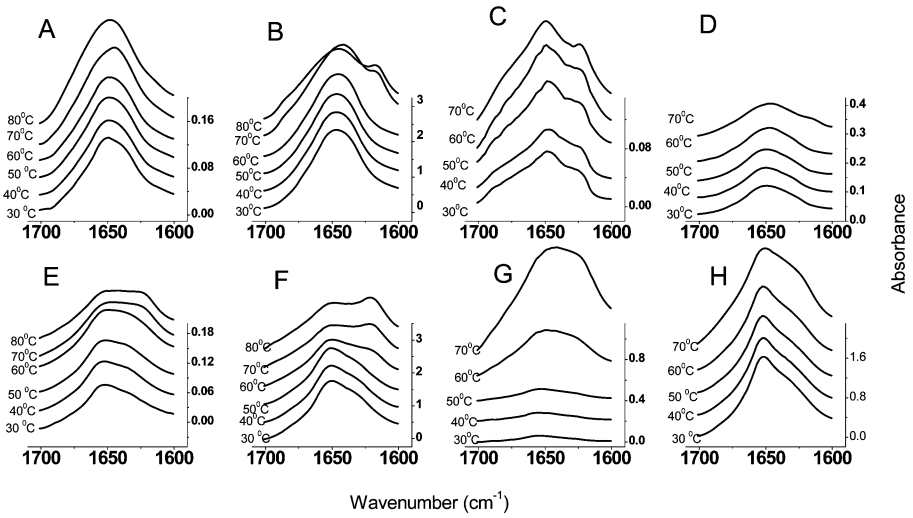

FIGURE 8: Comparison of secondary structure stabilities determined by ATR-FTIR of the four proteins. Amide I′ region of FTIR spectra as a function of temperature for lysozyme at 10 (A) and 400 mg/mL (B), amide I region for fibrinogen at 11 (C) and 59 mg/mL (D), amide I region for BSA at 12 (E) and 330 mg/mL (F), and amide I region for hemoglobin at 8 (G) and 245 mg/mL (H).

Both secondary and tertiary structure changes, however, occur at similar temperatures at high concentrations.

BSA. Concentrated BSA is destabilized by ~18 °C compared to that in dilute solutions (Figure 7C). Although precipitation complicated interpretation of these data at higher temperatures, it was still possible to obtain an undistorted signal at lower temperatures sufficient to reach this conclusion.

Fibrinogen. The CD-derived T_m of fibrinogen at 0.17 mg/mL is 47.5 °C, while that of fibrinogen at 59 mg/mL is 50 °C (Figure 7D). These data suggest that fibrinogen at high concentrations alters its secondary structure at slightly higher temperatures than in dilute solution.

CD Spectral Analysis

Although spectra of these proteins taken before heating suggest no direct effect of high protein concentration on secondary structure, CD spectra taken during thermal perturbation experiments exhibit very different signatures. Lysozyme in dilute solutions after thermal stress exhibits a peak minimum at 204 nm and a shoulder at 222 nm, indicating large increases in the amount of random coil mixed with residual helical structure (Figure 7E). At high concentrations, lysozyme has a single minimum that occurs at 210 nm. After their thermal transitions, spectra of hemoglobin, albumin, and fibrinogen in dilute solutions display peak minima at ~208 nm and shoulders at ~220 nm, a trend similar to that seen in dilute lysozyme solutions although with less disordered content (Figure 7F−H). At high concentrations and temperatures, spectra of hemoglobin, albumin, and fibrinogen display their peak minima at 221 nm (Figure 7F−H). These spectra suggest that, when thermally perturbed, the proteins in dilute solutions exhibit more disordered structures, while those in a more concentrated state manifest an increase in β-sheet structure content, probably intermolecular in nature (see below).

ATR-FTIR

FTIR spectroscopy was also employed in analyzing changes in secondary structure. The lowest concentration at which high-resolution spectra from all four proteins could be obtained was approximately 10 mg/mL. While this concentration is 50-fold higher than that used for the other techniques, it was still employed as the comparative low-concentration sample to provide another technique for probing the effect of concentration on secondary structure thermal stability. Potential alterations to the secondary structure of the proteins were monitored in the amide I or I′ region (1600−1700 cm^{-1}) of the IR spectra.

Lysozyme. The second-derivative spectrum of lysozyme in this spectral range consists primarily of a strong minimum at ca. 1649 cm^{-1} which is assigned to helical and coil structure (not illustrated). The position of this peak at "low concentrations" shifts from 1649 to 1647 cm^{-1} at higher temperatures (>60 °C), suggesting that the dominant component in the protein has shifted from helix to coil (Figure 8A). When a concentrated lysozyme solution is heated to 60 °C, the peak position begins to shift from its initial position at 1647 to 1645 cm^{-1} (Figure 8B). At a still higher temperature (70 °C), this peak is shifted further to 1641 cm^{-1} and a second peak that is highly characteristic of intermolecular β-sheet formation that was not observed in the melting of lysozyme at the lower concentration appears at ~1616 cm^{-1}.

The ratio of absorbances at 1649 and 1620 cm^{-1} does not change significantly over the entire temperature range at 10 mg/mL (Figure 9A). At 400 mg/mL, the onset of change is seen at ~60 °C, and the decrease in this ratio is significant (Figure 9A). Thus, it appears that lysozyme at high concentrations is less stable than in dilute solutions.

Fibrinogen. Fibrinogen at both high and low concentrations manifests a similar intermolecular β-sheet peak at 1624 cm^{-1} when heated, suggesting the presence of similar aggregated material (Figure 8C,D). On the basis of a ratio of the absorbance at 1647 and 1620 cm^{-1}, the T_m value of fibrinogen at 11 mg/mL is 42.5 °C, significantly lower than that of the protein at 59 mg/mL (50 °C, Figure 9B).

BSA. The intermolecular β-sheet peak at ~1618 cm^{-1} appears at 70 °C for BSA in dilute solutions and at 60 °C in the more concentrated solution (Figure 8E,F). A plot of the

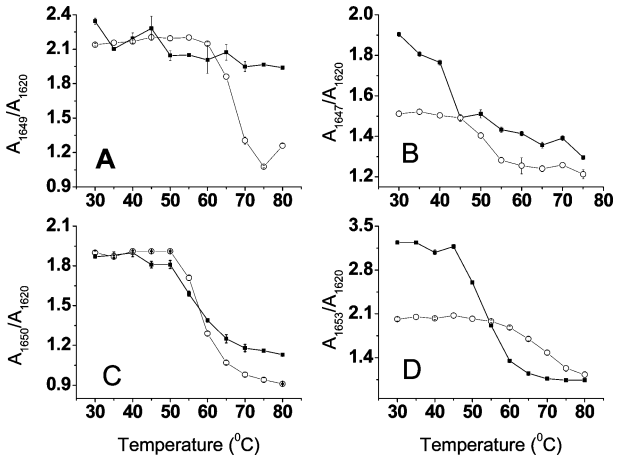

FIGURE 9: Ratio of absorbances as detected by ATR-FTIR of four proteins as a function of temperature: lysozyme [(A) (■) 10 and (○) 400 mg/mL], fibrinogen [(B) (■) 11 and (○) 59 mg/mL], BSA [(C) (■) 12 and (○) 330 mg/mL], and hemoglobin [(D) (■) 8 and (○) 245 mg/mL]. The error bars represent the standard error ($n = 3$). Error bars that are not visible are hidden within the symbol.

ratio of absorbances at 1650 and 1620 cm^{-1} as a function of temperature finds that the transition occurs at a similar temperature, i.e., 60 °C (Figure 9C).

Hemoglobin. At 60 °C, intermolecular β-sheet structure is formed in dilute hemoglobin solution (Figure 8G). At similar temperatures, there is no obvious aggregation at high concentrations (Figure 8H). Even up to 70 °C, the aggregation peak is still smaller at high concentrations than it is in dilute solutions. From the absorbance ratio of 1653 to 1620 cm^{-1}, the T_m value of the concentrated hemoglobin (65 °C) is 10 °C higher than that in dilute solution (55 °C) (Figure 9D). Therefore, hemoglobin at high concentrations is more stable and aggregates to a lesser extent. This seems to contradict the result observed by CD spectroscopy which suggests no difference in secondary structure between dilute and high concentrations. When hemoglobin in dilute solutions precipitates during its thermal transition, the secondary structure in solution seems to remain unchanged as monitored by CD spectroscopy, while the presumably adsorbed protein on the ATR may undergo an increase in the peak due to intermolecular β-sheet.

Differential Scanning Calorimetry

The thermal stability of the proteins at low and high concentrations was directly investigated by DSC. The differences in the observed T_m values correlate well with the structural changes seen in the spectroscopic measurements (Figure 10). At high concentrations, the T_m values of lysozyme and BSA are decreased by 4.5 and 20 °C, respectively, whereas the values for hemoglobin and fibrinogen increased by 8 and 3 °C, respectively.

Summary of the Transition Midpoints of the Four Proteins

Transition midpoints of the four proteins monitored by DSC, UV absorbance, OD_{350}, intrinsic fluorescence, and CD are summarized in Table 1. The lowest concentration used in the FTIR experiments is significantly higher than that used in other techniques, so the transition midpoints generated from FTIR are not included here. As confirmed by most of the techniques, lysozyme and BSA are destabilized by 2−20 °C while fibrinogen and hemoglobin are stabilized by 2−10 °C at high concentrations. Values for BSA at higher pH (6.8, near that used for the other proteins) are also included for the purposes of comparison. These results are quite different from those seen at the lower pH with in most cases (except the DSC measurements) much less destabilization observed.

DISCUSSION

The objective of these studies was to directly probe the effect of protein concentration on the colloidal and conformational stability of proteins by adapting conventional biophysical techniques for use with highly concentrated solutions. The impact of a high concentration on the colloidal and/or structural elements of protein stability has been a subject of speculation for some time, but little experimental literature is available that directly addresses this question. Thermal transition midpoints were obtained using various spectroscopic and calorimetric techniques to better characterize the various factors that determine protein stability at high concentrations. Four representative helix-rich proteins (lysozyme, hemoglobin, fibrinogen, and BSA) were employed for this purpose.

At 10 °C, both the secondary and tertiary structures appear similar if not identical for the four proteins over the entire range of concentrations that was examined. When the temperature is increased, however, the induced thermal transitions occur at different temperatures with apparently distinct unfolding and aggregation processes.

When considering protein stability, it is useful to recognize at least two different forms of this phenomenon in terms of the associative state of the particle (colloidal stability) and the integrity of the native fold (conformational stability). The hypothesis that these proteins undergo a reduction in volume through associative pathways is strongly supported by excluded volume theory (*4*). Lysozyme at high concentrations exhibits the predicted greater extent of aggregation upon heating. In contrast, fibrinogen demonstrates little effect due to the concentration on the temperature at which turbidity is initiated. Furthermore, hemoglobin is dramatically stabilized against association at higher concentrations ($\Delta T_m \sim 10$ °C). At pH 5.6, concentrated BSA gels at a much lower temperature (~15 °C) than that at which precipitation appears in dilute solution. At pH 6.8, concentrated BSA still gels, but in dilute solution, it does not aggregate over the entire temperature range that was studied. This strongly suggests that other factors also affect the colloidal stability. Because excluded volume theory is based on simple impenetrable molecular models and proteins are dynamic entities with complex surfaces, it is possible that protein surface effects could dominate excluded volume phenomena and could make significant contributions to colloidal stability. Although we have not studied the effect of pH in any detail, it is clear from the examination of BSA at two pH values that this variable can have a substantial effect on the differential colloidal stability of proteins as a function of concentration.

The impact of high concentration on the intrinsic structural stability of the proteins displays similar tendencies. The thermal stability of the secondary structure of lysozyme is found to decrease by 6 °C at high concentrations. The

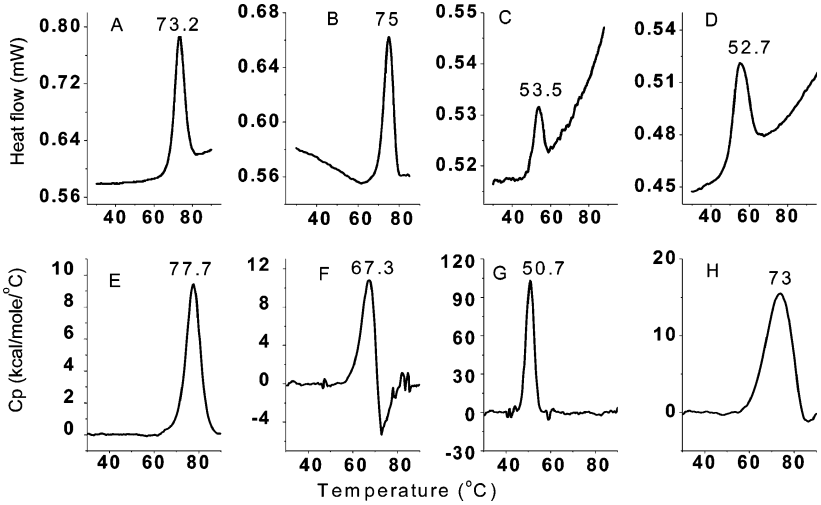

FIGURE 10: DSC thermograms of the four proteins: (A) lysozyme at 350 mg/mL, (B) hemoglobin at 245 mg/mL, (C) fibrinogen at 59 mg/mL, (D) BSA at 330 mg/mL, (E) lysozyme at 0.41 mg/mL, (F) hemoglobin at 0.3 mg/mL, (G) fibrinogen at 0.17 mg/mL, and (H) BSA at 0.27 mg/mL.

conformational stability of BSA is also found to be pH-dependent. At pH 5.6, concentrated BSA is destabilized by 18 °C. At pH 6.8, however, no significant difference in the T_m is observed between low and high concentrations. In the case of hemoglobin and fibrinogen, the thermal transitions of tertiary structure elements are stabilized by 2−10 °C in highly concentrated solutions. Furthermore, the formation of intermolecular β-sheet is less obvious in the concentrated hemoglobin solution. Since excluded volume effects are nonspecific, it may at first appear surprising that crowding seems to increase the conformational stability of some proteins at higher concentrations while have little effect on others. This can be simply explained as indicated above, however, by the simple idea that other factors such as the details of protein surface polarity and the kinetics of associative phenomena contribute significantly to the observed results.

No major changes in the hydrodynamic size of lysozyme and BSA are observed at the highest concentrations at lower temperatures. These results correlate with the fluorescence data, which indicate no change in the Trp environment and no self-association of these two proteins with concentration. Fibrinogen, the largest protein that was tested, exhibits a 50% increase in size, and its Trp residues manifest a 3 nm blue shift at high concentrations. This suggests some limited self-association or perhaps entanglement of fibrinogen in concentrated solutions at low temperatures. This could result in the tighter packing of fibrinogen's apolar core, which might contribute to the observed enhanced heat stability at high concentrations.

BSA gels at high concentrations when heated. The formation of this gel involves the formation of disulfide bonds (*34*). This process is pH- and concentration-dependent, diffusion-controlled, and transition-state-limited. These factors significantly complicate a better understanding of the stability of BSA at high concentrations.

While excluded volume effects no doubt contribute in part to the stability of proteins at high concentrations, it is certainly not unreasonable to expect that stability increases and decreases will be specific to individual proteins. For example, we found that using BSA in a slightly less pure state (96%) produces a species which displays much increased stability at higher concentrations compared to that of a more pure form (not illustrated). This could reflect the presence of trace quantities of ligands bound at this protein's apolar binding sites. At this point, the roles of pH, kinetics, protein dynamics, specific protein−protein interactions, solvent effects (*35*), and covalent alterations have yet to be sufficiently explored to accurately determine the extent of their effects on protein stability at higher concentrations. This work should provide a first experimental step, however, toward a better understanding of high protein concentration-based phenomena. There is also an important practical aspect of these studies. It is clear that quite simple modifications (or no modifications at all) of conventional techniques can be used to examine proteins at very high concentrations. This is of immediate utility in the analysis of highly concentrated protein-based pharmaceuticals since it should not be necessary to dilute actual drug formulations to test their identity and integrity.

ACKNOWLEDGMENT

We thank Dr. Sangeeta Joshi (The University of Kansas) for critical reading of preliminary drafts of the manuscript.

REFERENCES

1. Shire, S. J., Shahrokh, Z., and Liu, J. (2004) Challenges in the development of high protein concentration formulations, *J. Pharm. Sci. 93*, 1390−402.
2. Ross, P. D., and Minton, A. P. (1977) Analysis of non-ideal behavior in concentrated hemoglobin solutions, *J. Mol. Biol. 112*, 437−52.
3. Minton, A. P. (2005) Models for excluded volume interaction between an unfolded protein and rigid macromolecular cosolutes: Macromolecular crowding and protein stability revisited, *Biophys. J. 88*, 971−85.
4. Minton, A. P. (2000) Implications of macromolecular crowding for protein assembly, *Curr. Opin. Struct. Biol. 10*, 34−9.
5. Wilf, J., and Minton, A. P. (1981) Evidence for protein self-association induced by excluded volume. Myoglobin in the presence of globular proteins, *Biochim. Biophys. Acta 670*, 316−22.
6. Hall, D., and Minton, A. P. (2003) Macromolecular crowding: Qualitative and semiquantitative successes, quantitative challenges, *Biochim. Biophys. Acta 1649*, 127−39.

7. Sasahara, K., McPhie, P., and Minton, A. P. (2003) Effect of dextran on protein stability and conformation attributed to macromolecular crowding, *J. Mol. Biol. 326*, 1227−37.
8. Hatters, D. M., Minton, A. P., and Howlett, G. J. (2002) Macromolecular crowding accelerates amyloid formation by human apolipoprotein C-II, *J. Biol. Chem. 277*, 7824−30.
9. Rivas, G., Fernandez, J. A., and Minton, A. P. (2001) Direct observation of the enhancement of noncooperative protein self-assembly by macromolecular crowding: Indefinite linear self-association of bacterial cell division protein FtsZ, *Proc. Natl. Acad. Sci. U.S.A. 98*, 3150−5.
10. Zimmerman, S. B., and Minton, A. P. (1993) Macromolecular crowding: Biochemical, biophysical, and physiological consequences, *Annu. Rev. Biophys. Biomol. Struct. 22*, 27−65.
11. Minton, A. P., and Wilf, J. (1981) Effect of macromolecular crowding upon the structure and function of an enzyme: Glyceraldehyde-3-phosphate dehydrogenase, *Biochemistry 20*, 4821−6.
12. Minton, A. P. (1997) Influence of excluded volume upon macromolecular structure and associations in 'crowded' media, *Curr. Opin. Biotechnol. 8*, 65−9.
13. Minton, A. P. (2000) Effect of a concentrated "inert" macromolecular cosolute on the stability of a globular protein with respect to denaturation by heat and by chaotropes: A statistical-thermodynamic model, *Biophys. J. 78*, 101−9.
14. Tokuriki, N., Kinjo, M., Negi, S., Hoshino, M., Goto, Y., Urabe, I., and Yomo, T. (2004) Protein folding by the effects of macromolecular crowding, *Protein Sci. 13*, 125−33.
15. Tellam, R. L., Sculley, M. J., Nichol, L. W., and Wills, P. R. (1983) The influence of poly(ethylene glycol) 6000 on the properties of skeletal-muscle actin, *Biochem. J. 213*, 651−9.
16. Cole, N., and Ralston, G. B. (1994) Enhancement of self-association of human spectrin by polyethylene glycol, *Int. J. Biochem. 26*, 799−804.
17. Lindner, R., and Ralston, G. (1995) Effects of dextran on the self-association of human spectrin, *Biophys. Chem. 57*, 15−25.
18. Bryant, J. E., Lecomte, J. T., Lee, A. L., Young, G. B., and Pielak, G. J. (2005) Protein dynamics in living cells, *Biochemistry 44*, 9275−9.
19. Wang, D., Kreutzer, U., Chung, Y., and Jue, T. (1997) Myoglobin and hemoglobin rotational diffusion in the cell, *Biophys. J. 73*, 2764−70.
20. Nobbmann, U., Jones, S. W., and Ackerson, B. J. (1997) Multiple-Scattering Suppression: Cross Correlation with Tilted Single-Mode Fibers, *Appl. Opt. 36*, 7571−6.
21. Meyer, W. V., Cannell, D. S., Smart, A. E., Taylor, T. W., and Tin, P. (1997) Multiple-Scattering Suppresison by Cross Correlation, *Appl. Opt. 36*, 7551−8.
22. Provencher, S. W. (1979) Inverse Problems in Polymer Characterization: Direct Analysis of Polydispersity with Photon Correlation Spectroscopy, *Makromol. Chem. 180*, 201−9.
23. Provencher, S. W. (1982) A Constrained Regularization Method for Inverting Data Represented By Linear Algebraic or Integral Equations, *Comput. Phys. Commun. 27*, 229−42.
24. Provencher, S. W. (1982) Contin: A General Purpose Constrained Regularization Program for Inverting Noisy Linear Algebraic and Integral Equations, *Comput. Phys. Commun. 27*, 229−42.
25. Armstrong, J. K., Wenby, R. B., Meiselman, H. J., and Fisher, T. C. (2004) The hydrodynamic radii of macromolecules and their effect on red blood cell aggregation, *Biophys. J. 87*, 4259−70.
26. Liu, W., Cellmer, T., Keerl, D., Prausnitz, J. M., and Blanch, H. W. (2005) Interactions of lysozyme in guanidinium chloride solutions from static and dynamic light-scattering measurements, *Biotechnol. Bioeng. 90*, 482−90.
27. Kueltzo, L. A., Ersoy, B., Ralston, J. P., and Middaugh, C. R. (2003) Derivative absorbance spectroscopy and protein phase diagrams as tools for comprehensive protein characterization: A bGCSF case study, *J. Pharm. Sci. 92*, 1805−20.
28. Abugo, O. O., Nair, R., and Lakowicz, J. R. (2000) Fluorescence properties of rhodamine 800 in whole blood and plasma, *Anal. Biochem. 279*, 142−50.
29. Eisenger, J., and Flores, J. (1979) Front-face fluorometry of liquid samples, *Anal. Biochem. 94*, 15−21.
30. Kueltzo, L. A., and Middaugh, C. R. (2003) Structural characterization of bovine granulocyte colony stimulating factor: Effect of temperature and pH, *J. Pharm. Sci. 92*, 1793−804.
31. Vivian, J. T., and Callis, P. R. (2001) Mechanisms of tryptophan fluorescence shifts in proteins, *Biophys. J. 80*, 2093−109.
32. Lakowicz, J. R. (1999) *Principles of fluorescence spectroscopy*, 2nd ed., Kluwer Academic/Plenum Publishers, New York.
33. Schwinte, P., Voegel, J. C., Picart, C., Haikel, Y., Schaaf, P., and Szalontai, B. (2001) Stabilizing effects of various polyelectrolyte multilayer films on the structure of adsorbed/embedded fibrinogen molecules: An ATR-FTIR study, *J. Phys. Chem. B 105*, 11906−16.
34. Vaiana, S. M., Emanuele, A., Palma-Vittorelli, M. B., and Palma, M. U. (2004) Irreversible formation of intermediate BSA oligomers requires and induces conformational changes, *Proteins 55*, 1053−62.
35. Sorin, E. J., and Pande, V. S. (2006) Nanotube confinement denatures protein helices, *J. Am. Chem. Soc. 128*, 6316−7.

BI060525P